for their help in obtaining the laser flash photolysis data.

References

1. Y. V. Korshak, A. A. Ovchinnikov, A. M. Shapino, T. V. Medvedeva, and V. N. Spector, *JEPT Lett (Engl. Transl.)*, **43**, 399 (1986); I. Fujita, T. Yoshio, T. Takeji, T. Kinoshita, and K. Itoh, *J. Am. Chem. Soc.*, **112**, 4074 (1990); J. B. Torrance, S. Oostra, and A. Nazzal, *Synth. Met.*, **19**, 709 (1987); J. S. Miller, A. J. Epstein, and W. M. Reiff, *Chem. Rev.*, **88**, 207 (1988).
2. Y. Teki, T. Takui, K. Itoh, H. Iwamura, and K. Kobayashi, *J. Am. Chem. Soc.*, **108**, 2147 (1986).
3. H. Iwamura, *Adv. Phy. Org. Chem.*, **26**, 180 (1990).
4. W. T. Borden, "Diradicals", Wiley, New York Chap 1, (1982).
5. D. Bethell and M. R. Brinkman, *Adv. Phy. Org. Chem.*, **10**, 53 (1973).
6. A. R. Lepley and G. L. Closs, "*Chemically Induced Magnetic Polarization*" Willy, New York (1973).
7. E. Wasserman, R. W. Murray, W. A. Yager, A. M. Trozzolo, and G. Smolinsky, *J. Am. Chem. Soc.*, **89**, 5076 (1967).
8. J. Brickman and G. Kothe, *J. Chem. Phys.*, **59**, 2807 (1973); T. Takui and K. Itoh, *Chem. Phys. Lett.*, **50**, 1251 (1978).
9. N. Mataga, *Theor. Chim. Acta.*, **10**, 372 (1968); A. A. Ovchinnikov, *Theor. Chim. Acta.*, **47**, 297 (1978); M. Schwoerer, R. A. Huber, and W. Hartl, *Chem. Phys. Lett.*, **55**, 97 (1981).
10. T. Takui and K. Itoh, *Chem. Phys. Lett.*, **19**, 120 (1973); K. Itoh, *Pure. Appl. Chem.*, **50**, 1251 (1978); Y. Teki, T. Takui, H. Yagi, K. Itoh, and H. Iwamura, *J. Chem. Phys.*, **83**, 539 (1985); S. Murata, T. Sugawara, and H. Iwamura, *J. Am. Chem. Soc.*, **109**, 1266 (1987).
11. R. W. Murray and M. L. Kaplan, *J. Am. Chem. Soc.*, **88**, 3527 (1966); H. Meier and I. Menzer, *Synthesis*, 215 (1971).
12. E. C. Evers and A. G. Knox, *J. Am. Chem. Soc.*, **73**, 1739 (1951).
13. T. C. Hess, Ph. D. Dissertation, University of California, Los Angeles, CA (1978).
14. C. L. Kreil, Ph. D. Dissertation, University of California, Los Angeles, CA (1983).
15. K. Itoh, *Pure. Appl. Chem.*, **50**, 1251 (1978); H. Iwamura, *Pure. Appl. Chem.*, **59**, 1595 (1987).
16. K. Itoh, *Chem. Phys. Lett.*, **1**, 235 (1967).
17. H. Tomioka, H. Okuno, and Y. Izawa, *J. Org. Chem.*, **45**, 5278 (1980); H. Tomioka, M. Kondo, and Y. Izawa, **46**, 1090 (1981).
18. J. Kopecky, "*Organic Photochemistry*: A Visual Approach", VCH Publishers, Inc., 33 (1992).
19. For reviews of the photochemistry of diazo compound, see: (a) H. Dürr, In "*Methoden der Organicschen Chemie (Houben-Weyl)*." G. Thieme: Stuttgart, **Vol. 4/5b**, 1158 (1975); (b) H. Dürr, *Topics Curr. Chem.*, **55**, 87 (1976); (c) M. Regitz and G. Maas, "*Diazo compounds: Properties and Synthesis*", Academic, New York (1986); (c) Y. Z. Li and G. B. Schuster, *J. Org. Chem.*, **52**, 4460 (1987).
20. (a) H. Meier and K. P. Zeller, *Angew. Chem. Int. Ed. Engl.*, **14**, 32 (1975); (b) W. Ando, In "*The Chemistry of the Diazonium and Diazo Group*", S. Patai ed., Wiley, New York, Part 1, 458 (1978); (c) M. Regitz and G. Mass, "*Diazo compounds: Properties and Synthesis*", Academic Press, Orlando, Florida, 185 (1986).
21. C. Marfisi, P. Verlaque, D. Davidovics, J. Pourcin, L. Pizzala, J.-P. Acard, and H. Bodot, *J. Org. Chem.*, **48**, 533 (1983).
22. W. J. Bouma, R. H. Nobes, L. Radom, and C. E. Woodward, *J. Org. Chem.*, **47**, 1869 (1982).
23. S.-J. Chang, B. K. Ravi Shankar, and H. Shechter, *J. Org. Chem.*, **47**, 4226 (1982).

Observation of Electronic Emission Spectra of CH_3S

Sang Kuk Lee

Department of Chemistry, College of Natural Sciences, Pusan National University, Pusan 609-735

Received January 13, 1993

The combination of Fourier Transform spectroscopy with a technique of supersonic expansion has been employed to examine the vibronic structure of the transition $A^2A_1 \rightarrow X^2E$ of CH_3S radical. CH_3S was produced by an electric *dc* discharge of the precursor $(CH_3)_2S$. The emission spectrum of CH_3S shows extensive progressions of CS stretching frequencies in the transitions. The molecular parameters describing the vibrational structure of CH_3S have been determined with high accuracy from the analysis of the emission spectrum.

Introduction

For a long time, alkylthio radicals (RS ·) have been reported[1-3] to be an intermediate in combustion and atmospheric chemistry of organosulfur compounds. Theses compounds also play an important role in the atmospheric sulfur cycle and contribute to the acidic rain problem. Particularly, CH_3S is considered an important intermediate in oxidative reaction

of CH_3SCH_3, CH_3SSCH_3, and CH_3SH, which may be related to the air pollution in the atmosphere.[4]

From the spectroscopic point of view, CH_3S has many interesting features. It has a ^2E ground electronic state and thus is subjected to the Jahn-Teller distortion. CH_3S has a relatively large spin-orbit interaction compared to its counterpart CH_3O.[5] Thus, an accurate determination of the magnitudes of the spin-orbit interaction and the Jahn-Teller distortion is very interesting.[6] In addition, it provides a good opportunity to examine the interaction between the Jahn-Teller distortion and the spin-orbit splitting.

Until now, CH_3S has been investigated by serveral spectroscopic methods including emission,[5] microwave,[7], matrix infrared,[8] electronic paramagnetic resonance,[9] laser photodetachment[10,11] and laser induced fluorescence.[12,13] The emission experiment estimated the possible position of the band origin of the transition $A^2A_1 \rightarrow X^2E$ of CH_3S.[5] The LIF experiment[12] could determine the lifetime at given vibronic states. In addition to its lifetime measurement, the vibrational structure of CH_3S was analyzed from the fluorescence dispersion spectra. On the other hand, high resolution LIF experiment[13] employing a supersonic expansion system resolved the rotational structure of the transition $A^2A_1 \rightarrow X^2E$ of CH_3S and could obtain the molecular parameters at the ground and the excited electronic states.

However, to our surprise, there has been no extensive studies on the vibrational progressions of CH_3S in the ground and the excited electronic states. In this paper, we report the vibrational frequencies of the transition $A^2A_1 \rightarrow X^2E$ of CH_3S from the analysis of the emission spectrum obtained with a FT-spectrometer combined with a supersonic expansion system.

Experimental

CH_3S is a very unstable molecule and does not exist in the normal condition. Thus, it has been usually produced[5] by photolyzing a geometrically ideal precursor dimethyl disulfide, CH_3SSCH_3 by using strong radiation sources such as excimer lasers.[12]. However, an electric *dc* discharge of this precursor generates a large amount of S_2 molecule due to the easy cleavage of C-S bond rather than CH_3S radical. On the other hand, another precursor methyl sulfide, CH_3SCH_3 can be used for the generation of CH_3S by an electric *dc* discharge without producing S_2.

Figure 1 shows the experimental setup which is similar to those used previously.[14] CH_3S radical was produced from the mixture of He buffer gas and the precursor $(CH_3)_2S$[He : $(CH_3)_2S = 100 : 1$] with an electric *dc* discharge in the supersonic expansion system. For the supersonic expansion system, 2 atm pressure of the gas mixture has been expanded through 0.2 mm diameter of nozzle into an expansion chamber which was made of 6-way cross Pyrex glass tube of 5.0 cm in diameter, and was maintained by a mechanical vacuum pump and a boost pump to less than 1.0 Torr of pressure. The nozzle was made by a glass capillary of thick wall, narrowed at one end to provide the desired hole size. The anode was a 2 mm diameter of stainless steel rod sharpened at the tip and inserted into the capillary through an O-ring to within 1 mm of the orifice. The copper pipe of 7.5 cm in diameter connecting the expansion to the pump

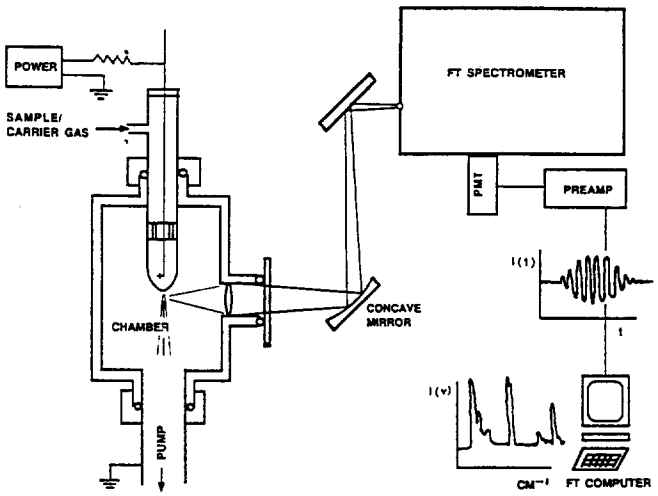

Figure 1. Schematic diagram of the experimental apparatus used for this work.

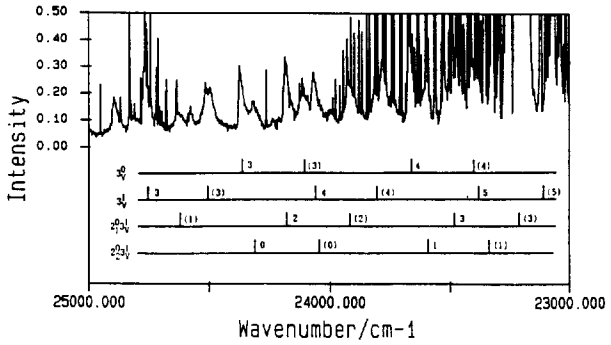

Figure 2. A portion of the CH_3S spectrum obtained with the FT-spectrometer at the resolution of 2.0 cm^{-1}. The numbers without parenthesis and with parentheses indicate the vibrational quantum numbers of the transitions $^2A_1 \rightarrow ^2E_{3/2}$ and $^2A_1 \rightarrow ^2E_{1/2}$, respectively.

was used as the cathode at the ground potential. The distance between the two electrodes was about 30 cm. The typical operating condition was about 5 mA discharge current and 3.0 KV of *dc*. The discharge was stabilized by using a 250 KΩ of current-limiting ballast resistor. With this operating conditions, we were able to obtain the rotational temperature to $T_{rot} = \sim 50$ K according to a theoretical calculation of the intensity distribution of the rotational spectrum.[15] The discharge emission from an area of the jet below the nozzle orifice was focussed with several optics onto the emission port of a FT-spectrometer (Bruker model IFS120HR) and was detected with a PMT (Hamamatsu model 1P28). The optical alignment of the spectrometer was optimized by adjusting the position of the beamsplitter and the fixed mirror.

Since the emission from the He gas and fragment molecules, mostly CH radical in this case is much stronger than that of CH_3S, an optical filter of a suitable spectral range (Corning model number 5-57) was used to block off the unwanted emission. The color filter used for this purpose has spectral window range of about 18000-30000 cm^{-1}. Typically, 1000 spectra were averaged over 30 min to obtain the final emission spectrum shown in Figure 2 at the resolution of

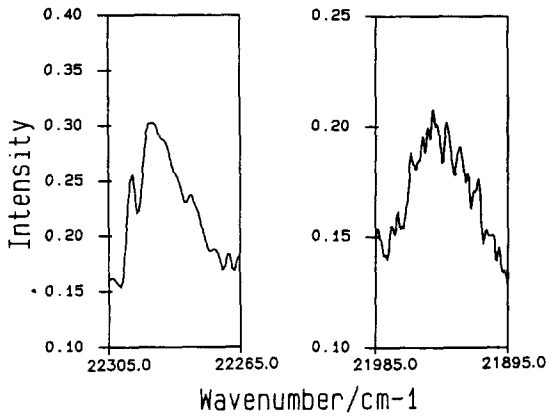

Figure 3. Typical bandshape exemplified by the CH_3S spectrum. The band having bandhead in the right side is from the $^2A_1 \rightarrow {}^2E_{3/2}$ (3_8^0) transition and the other having more symmetric shape in the left side is from $^2A_1 \rightarrow {}^2E_{1/2}$ ($2_2^0 3_3^1$) transition.

2 cm^{-1}. The frequency of the spectrometer was calibrated with the I_2 transitions in the I_2 atlas[16] and believed to be better than 0.01 cm^{-1} in this spectrum.

The O_0^0 bandhead of the transition $^2A_1 \rightarrow {}^2E_{3/2}$ of CH_3S was reported by Suzuki *et al.*[12] to be located at 26530 cm^{-1}. Since this experiment is to obtain the emission spectrum of CH_3S, which must lie in the lower frequency region of the band origin, the spectrum region from 17000 to 32000 cm^{-1} was scanned.

Results and Discussion

Figure 2 shows a portion of CH_3S emission spectrum obtained with the FT-spectrometer at the resolution of 2 cm^{-1}. Most of CH_3S bands are found in the range of 20000-27000 cm^{-1}. In some frequency regions, CH_3S bands are heavily overlapped with the peaks of CH. The peaks of CH at 23200 and 25600 cm^{-1} are from the transitions of $A^2\Delta \rightarrow X^2\Pi$ and $B^2\Sigma^- \rightarrow X^2\Pi$, respectively.[17] Since the CH and He peaks appears as sharp and strong compared to those of CH_3S, we have no problem in distinguishing the CH_3S bands from those of CH and He. The molecular radical CH was produced from the precursor $(CH_3)_2S$ by electric discharge in the decomposing process. The He peaks are from the buffer gas. The position of the maxima of CH_3S bands was measured within $\pm$ 0.1 cm^{-1}. In the emission of CH_3S, the characteristics of the doublet bands are attributed to the transitions of $^2A_1 \rightarrow {}^2E_{3/2}$ and $^2A_2 \rightarrow {}^2E_{1/2}$, respectively. Thus, the interval between the doublet bands are easily identified as the spin-orbit splitting ($^2E_{3/2}$, $^2E_{1/2}$) of the ground electronic state. The tentative assignment of the bands has been made with the LIF data[12] on this molecule. Since the emission spectrum, in general, is much more complicated compared to the LIF spectrum, the bands with weak intensity have been analyzed by using the Hamiltonian[7] shown below

$$F'(v_3') = T_e + \omega_3'(v_3' + 0.5) - \omega_3' x_3'(v_3' + 0.5)^2 \quad \text{for } {}^2A_1 \text{ state}$$

$$F''(v_2'', v_3'') = \omega_3''(v_3'' + 0.5) - \omega_3'' x_3''(v_3'' + 0.5)^2 + \omega_2''(v_2'' + 0.5) - \omega_2'' x_2''(v_2'' + 0.5)^2 + \omega_{23}'' x_{23}''(v_2'' + 0.5)(v_3'' + 0.5) \quad \text{for } {}^2E_{3/2} \text{ state}$$

Table 1. CH_3S Band Positions and Assignments[a]

$^2A_1 \rightarrow {}^2E_{3/2}$	$^2A_1 \rightarrow {}^2E_{1/2}$	Assignments[b]
Position (cm^{-1})	Position (cm^{-1})	
25800.4	N.O.	3_1^0
25080.4	24818.5	3_2^0
24371.7	24111.6	3_3^0
23668.5	23408.1	3_4^0
22974.2	22713.2	3_5^0
22292.0	22032.0	3_6^0
21619.8	21358.6	3_7^0
20956.1	N.O.	3_8^0
26200.9	25936.0	3_1^1
25479.9	25218.4	3_2^1
24769.0	24509.7	3_3^1
24069.6	23810.2	3_4^1
23375.0	N.O.	3_5^1
22692.9	N.O.	3_6^1
22020.1	21757.4	3_7^1
26597.5	26337.8	3_1^2
25876.1	25617.9	3_2^2
25166.3	24905.8	3_3^2
25218.4	24957.6	2_1^0
24496.3	24235.5	$2_1^0 3_1^0$
23782.7	23522.3	$2_1^0 3_2^0$
23079.6	22820.7	$2_1^0 3_3^0$
22386.5	22126.5	$2_1^0 3_4^0$
21700.1	21440.6	$2_1^0 3_5^0$
21027.2	20763.0	$2_1^0 3_6^0$
20360.1	20100.1	$2_1^0 3_7^0$
25617.9	N.O.	$2_1^0 3_0^1$
24895.1	24634.7	$2_1^0 3_1^1$
24183.4	23923.4	$2_1^0 3_2^1$
23478.8	23217.3	$2_1^0 3_3^1$
22785.0	22525.3	$2_1^0 3_4^1$
23917.4	23658.5	2_2^0
22497.0	22235.9	$2_2^0 3_2^0$
21800.6	21541.7	$2_2^0 3_3^0$
21114.2	20854.9	$2_2^0 3_4^0$
20437.9	20178.6	$2_2^0 3_5^0$
19769.3	19508.9	$2_2^0 3_6^0$
24317.7	24057.3	$2_2^0 3_0^1$
23602.3	N.O.	$2_2^0 3_1^1$
22896.0	22636.5	$2_2^0 3_2^1$
22200.5	21942.0	$2_2^0 3_3^1$
21514.1	N.O.	$2_2^0 3_4^1$
23030.0	N.O.	$2_3^0 3_0^1$
22319.9	22060.0	$2_3^0 3_1^1$
21619.8	21358.6	$2_3^0 3_2^1$

[a] N.O. stands for no observation due to the weak intensity or overlap. [b] The assignment 3_1^0 means the transition of the v_3 vibrational mode from $v=0$ at the upper electronic state ($^2A_1$) to $v=1$ at the ground electronic state (^2E).

From these analyses, a total of 45 and 37 vibrational peaks belonging to the progressions of 4 fundamental and 5 combi-

Table 2. Determined Parameters and Spin-Orbit Coupling Constant (A) of CH_3S[a]

Parameters	This work[b]	Previous Work[c]
T_e	27360.02(47)	27332.59
ω_3'	402.68(101)	410.0
$\omega_3'x_3'$	1.44(38)	3.44
ω_3''	742.98(24)	744.8
$\omega_3''x_3''$	4.72(3)	5.45
ω_2''	1326.83(71)	1322.3
$\omega_2''x_2''$	5.56(19)	3.32
$\omega_{23}''x_{23}''$	−7.40(8)	−8.5
A	260.4± 2.0	−255.5[d]
Number of data	45	24

[a] in units of cm^{-1}. [b] Number in parenthesis is one standard error in units of last digit in the parameter. [c] References (12). [d] Reference (13).

national bands has been identified in each electronic transition $^2A_1 \rightarrow {}^2E_{3/2}$ and $^2A_1 \rightarrow {}^2E_{1/2}$, respectively. Table 1 lists the frequencies and assignments of the CH_3S bands observed in the emission spectrum. With the accurate measurement of the positions of the peak maxima, we have found that the differences in frequencies between $^2A_1 \rightarrow {}^2E_{3/2}$ and $^2A_1 \rightarrow {}^2E_{1/2}$ are nearly constant over the whole range observed. It turned out that the intensity of the transition $^2A_1 \rightarrow {}^2E_{1/2}$ is weaker than that of the $^2A_1 \rightarrow {}^2E_{3/2}$.

The molecule, CH_3S has the ^2E ground elecronic state ($^2E_{1/2}$ and $^2E_{3/2}$) and a relatively large spin-orbit splitting. The spin-orbit interaction has been estimated to be about -280 ± 20 cm^{-1} by LIF method[5,12], -221.0 ± 2.0 cm^{-1} by microwave spectroscopy,[18] and -255.5 cm^{-1} by very low temperature LIF method.[13] In this work, the spin-orbit coupling constant (A) has been determined to be -260.4 ± 2.0 cm^{-1} from the differences in the frequencies between $^2A_1 \rightarrow {}^2E_{3/2}$ and $^2A_1 \rightarrow {}^2E_{1/2}$. The value obtained in this work agrees well with the result of the previous work[13] employing LIF method. The final vibrational parameters by the least squares fit to the Hamiltonian shown above are summarized in Table 2. With these parameters, the positions of the observed bands could be predicted within a few wavenumbers. Also, it is interesting to note that the value of A for CH_3S is smaller than that for SH (-377 cm^{-1}).[13] The trend is same as the case of CH_3O (-62 cm^{-1})[19] and OH (-139 cm^{-1}).[20]

In addition, it has been shown in Figure 3 that the bandshape for the $^2A_1 \rightarrow {}^2E_{3/2}$ transition is quite different from that for $^2A_1 \rightarrow {}^2E_{1/2}$. The former shows clear bandheads with red degradation and the latter exhibits broader and more symmetric peaks. This means that the molecular structures in the $^2E_{3/2}$ and $^2E_{1/2}$ states are different, and that the rotational constant of the $^2E_{1/2}$ levels is close to that of the excited $^2A_1$ state. Since, according to the Franck-Condon principle, the variation of peak intensities reflects the bond length at both states connected by the transition, the structure in the excited state can be estimated if we know the structure in the ground state and the intensity variation over the transition quantum numbers. The structure in the ground electronic state was already determined by using microwave spectroscopy on this molecule.[7] The analysis of the intensity distribution of the vibronic transition in the emision spectrum is now is progress.

Conclusion

The emission spectrum of CH_3S has been obtained with an FT-spectrometer coupled with a supersonic expansion system. The spectrum shows vibrational progression of the fundamental and combinational bands in the frequency range of 20000-27000 cm^{-1}. The bands observed have been extensively assigned. The harmonic frequencies and anharmonic constant of the bands have been determined in the ground and the excited electronic states. Also the spin-orbit coupling constant (A) in the ground electronic state has also been estimated to be $A=-260.4$ cm^{-1}. With these parameters, we could predict the positions of vibrational peaks within a few wavenumber.

Acknowledgement. This work was supported by the Korea Science and Engineering Foundation (Grant No. 923-0300-007-2). The author thanks The Ohio State University for letting use the FT-spectrometer (Bruker IFS120HR).

References

1. S. Hatakeyama and H. Akimoto, *J. Phys. Chem.*, **87**, 2387 (1983).
2. H. Niki, P. D. Maker, C. M. Savage, and L. P. Breitenbach, *Int. J. Chem. Kinet.*, **15**, 647 (1983).
3. D. Grosjean and R. Lewis, *Geophys. Res. Lett.*, **9**, 1203 (1982).
4. See the references given by A. Mellouki, J. L. Jourdain, and G. LeBras, *Chem. Phys. Lett.*, **148**, 231 (1988).
5. K. Ohbayashi, H. Akimoto, and I. Tanaka, *Chem. Phys. Lett.*, **52**, 47 (1977).
6. S. D. Brossard, P. G. Carrick, E. L. Chappell, S. C. Hulegaard, and P. C. Engelking, *J. Chem. Phys.*, **84**, 2459 (1986).
7. Y. Endo, S. Saito, and E. Hirota, *J. Chem. Phys.*, **81**, 122 (1984).
8. M. E. Jacox, *Can. J. Chem.*, **61**, 1306 (1983).
9. T. Gillbro, *Chem. Phys.*, **4**, 476 (1974).
10. P. C. Engelking, G. B. Ellision, and W. C. Lineberger, *J. Chem. Phys.*, **69**, 1826 (1978).
11. B. K. Janousek and J. I. Brauman, *J. Chem. Phys.*, **72**, 694 (1980).
12. M. Suzuki, G. Inoue, and H. Akimoto, *J. Chem. Phys.*, **81**, 5405 (1984).
13. Y.-C. Hsu, X. Liu, and T. A. Miller, *J. Chem. Phys.*, **90**, 6852 (1989).
14. M. H. Suh, S. K. Lee, B. D. Rehfuss, T. A. Miller, and V. E. Bondybey, *J. Phys. Chem.*, **95**, 2727 (1991).
15. S. K. Lee, unpublished data on CN emission.
16. S. Gerstenkorn and P. Luc, "Atlas du Spectre d'Absorption de la Molecule d'Iodide", Editions du Centre National de la Recherche Scientifique, Paris, 1978; *Rev. Phys. Appl.*, **14**, 791 (1979).
17. K. P. Huber and G. Herzberg, Molecular Spectra and Molecular Structure, Part IV, pp. 140, Van Nostrand Reinhold, New York, 1979.

18. Y. Endo, S. Saito, and E. Hirota, *J. Chem. Phys.*, **85**, 1770 (1986).
19. X. Liu, C. P. Damo, T.-Y. D. Lin, S. C. Foster, P. Misra, L. Yu, and T. A. Miller, *J. Phys. Chem.*, **93**, 2266 (1989).
20. J. M. Brown, M. Kaise, C. M. Kerr, and D. J. Milton, *Mol. Phys.*, **36**, 553 (1978).

The Electronic Structure and Chemical Bonding between Metal and Oxygen Atoms: Tl22-Based Copper Oxide Superconductors

Man Shick Son and U-Hyon Paek*

Department of Chemistry, Kyeongsang National University, Chinju 660-701
Received September 30, 1992

Using tight-binding molecular orbital methods for charged cluster models, we studied the electronic structrue and chemical bonding of thallium-oxygen and copper-oxygen atoms in Tl22-based copper oxide. The interaction between the s orbital of Tl atom and the p_x and p_y orbitals of $O3_{eq}$ atom in the Tl layers results in nonbonding. The interaction between the s orbital of Tl atom and the p_z orbital of O2 and $O3_{ax}$ atoms in Ba and Tl layers results in antibonding. The interaction between the d_{z^2} orbital of Cu atom and the p_z orbital of O2 atom also results in antibonding. The Tl22-based copper oxide superconductors can be understood in terms of a local electron transfers from Cu layers to Tl layers along c-direction. The resulting electron transfers have the same patterns as those of $YBa_2Cu_3O_7$ and $YBa_2Cu_4O_8$ superconductors.

Introduction

At present Tl-based copper oxide superconductors show the highest superconducting transition temperatures T_c[1-5]. The Tl-based copper oxide superconductors have Cu perovskite-like unit structures. These compounds can be divided into two types according to the space group. Type I that is Tl12-based copper oxide superconductors has space group P4/mmm. Type II that is Tl22-based copper oxide supeconductors has the space group I4/mmm. The ideal superconducting phases of Tl12-based and Tl22-based copper oxide superconductors may be classified into six groups, $TlBa_2CaCu_2O_7$(Tl1212 system)[6], $TlBa_2Ca_2Cu_3O_{10}$(Tl1223)[7], $TlBa_2Ca_3Cu_4O_{11}$(Tl1234)[8], $Tl_2Ba_2CuO_6$(Tl2201)[3], $Tl_2Ba_2CaCu_2O_8$(Tl2212)[4], and $Tl_2Ba_2Ca_2Cu_3O_{10}$(Tl2223)[5].

The structures of these systems are separated by Tl-O monolayer and Tl-O bilayers for Tl12-based and Tl22-based copper oxide superconductors. Figure 1 shows nominal unit cells[9] for Tl2201, Tl2212, and Tl2223 superconductors. Ca^{2+} cations are between adjacent Cu layers and Ba^{2+} cations between Cu layers and Tl layers. From the comparison of the crystal structures of $YBa_2Cu_3O_7$ and Tl22-based copper oxide superconductors, copper-oxygen chains are present in a $YBa_2Cu_3O_7$ superconductor, while these chains are absent in Tl22-based copper oxide superconductors.

Using ASED-MO[10] of the tight-binding molecular orbital method, we studied electronic structures and chemical bonding of the thallium-oxygen and copper-oxygen atoms for Tl 22-based copper oxide superconductors.

The Cluster Size and Calculation Methods

The oxygen atoms in different layers of superconductors are crystallographically ineqivalent. Tl22-based copper oxide superconductors are labeled by O1 (in Cu layers), O2 (in Ba layers), and O3 (in Tl layers). The atoms in the two inequivalent Cu layers are labeled Cu, O1, Cu′ and O1′. These labels are shown in Figure 1. We also use atoms $O3_{eq}$ and $O3_{ax}$ which stand for equatorial and axial positions in the Tl double layer for Tl22-based copper oxide superconductors.

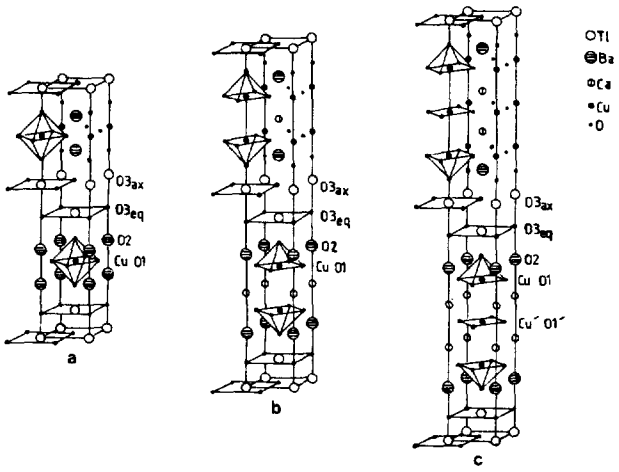

Figure 1. Nominal unit cells for $Tl_2Ba_2CuO_6$, $Tl_2Ba_2CaCu_2O_8$, and $Tl_2Ba_2Ca_2Cu_3O_{10}$ superconductors. (a) $Tl_2Ba_2CuO_2$ superconductors. (b) $Tl_2Ba_2CaCu_2O_8$ superconductor. (c) $Tl_2Ba_2Ca_2Cu_3O_{10}$ superconductors.

Freeman *et al.*[11] and Kasowski *et al.*[12] calculated the band structure and electronic structure using the band theory for Tl22-based copper oxide superconductors. Their findings indicate that the Tl and Cu layers affect Fermi energy states. Using the full-potential linearized augmented plane-wave